Journal of Applied Physics

RESEARCH ARTICLE | AUGUST 02 2024

Mode transitions in a magnetically shielded Hall thruster. I. Experimentally informed model

Benjamin A. Jorns ; Ethan Dale ; Richard R. Hofer

J. Appl. Phys. 136, 053301 (2024)
https://doi.org/10.1063/5.0205983

AIP Publishing

Journal of Applied Physics ARTICLE pubs.aip.org/aip/jap

Mode transitions in a magnetically shielded Hall thruster. I. Experimentally informed model

Cite as: J. Appl. Phys. **136**, 053301 (2024); doi: 10.1063/5.0205983
Submitted: 28 February 2024 · Accepted: 10 July 2024 ·
Published Online: 2 August 2024

View Online Export Citation CrossMark

Benjamin A. Jorns,[1,a)] Ethan Dale,[1] and Richard R. Hofer[2]

AFFILIATIONS

[1]Department of Aerospace Engineering, University of Michigan, Ann Arbor, Michigan 48109, USA
[2]Jet Propulsion Laboratory, California Institute of Technology, Pasadena, California 91011, USA

[a)]**Author to whom correspondence should be addressed:** bjorns@umich.edu

ABSTRACT

An experimental evaluation is presented of a two-equation model for the low frequency (<25 kHz), large amplitude (>100% of mean) discharge oscillations exhibited by a 9-kW class magnetically shielded Hall thruster. The model is based on a theoretical treatment of the "breathing mode" oscillations in Hall thrusters (Barral and Peradzyński, "A new breath for the breathing mode," IEPC-2009-070) and includes governing equations for fluctuations in the discharge current and the spatially averaged neutral density in the thruster channel. The derivation of the governing equations is reviewed, and the key simplifying assumptions are formulated in terms of comparisons between the magnitudes of relative fluctuations in spatially averaged plasma properties. Experimental measurements are performed of these plasma properties at an operating condition of 300 V discharge voltage and 10 A discharge current. It is found that all quantities of interest such as drift speed, electric field, and temperature fluctuate on the timescale of the low frequency oscillations. However, the relative phasing of these properties combine in such that the key assumptions of the model are satisfied—all but the neutral density and discharge fluctuations can be neglected in the equations for neutral density and current oscillations. A physical interpretation of the validity of the assumptions is presented, and the model is discussed in the context of its extensibility to other operating conditions. The validated model forms the basis for a parametric study presented in Part II of mode transitions and the criterion for these transitions in a magnetically shielded Hall thruster.

I. INTRODUCTION

The extended lifetime of magnetically shielded Hall thrusters[1–3] combined with their high specific impulse (>2000 s) and moderate thrust density (>10 N/m^2) is an enabling feature for a wide range of interplanetary missions. To meet the requirements of the most demanding, scientifically compelling missions, these shielded thrusters also must be capable of maintaining high performance (efficiency and specific impulse) as the input power and current decrease. This stems from the fact that as a spacecraft spirals from the sun, the solar power available to the propulsion system falls. This requirement poses a challenge for magnetically shielded thrusters as it has been found in some of these devices that if they are throttled below ∼60% of their nominal design current at high discharge voltage (>600 V)/high specific impulse (>2500 s), they can undergo a mode transition characterized by large amplitude (>100% background) and high frequency (∼10–50 kHz) oscillations in the discharge current and power.[4,5] These large scale oscillations could cause a potential risk to the thruster health or the spacecraft. In light of this challenge and the advantages of magnetically shielded thrusters with high-specific impulse for deep space applications, there is a need to understand this mode transition and mitigate it.

The frequency and amplitude of the mode transition exhibited at low current in shielded thrusters suggest that it may be a strong manifestation of the classical breathing mode oscillation.[6,7] This instability appears in nearly all Hall thrusters and has been the subject of extensive numerical[8–29] and experimental study.[30–48] The conventional description of this oscillation[8] is that it is related to ionization in the Hall thruster channel. The neutral and plasma density in this region follow a predator–prey cycle that results in large amplitude (∼20%–100% background), low-frequency (∼10–50 kHz) periodic fluctuations in the discharge current. The similarities between these fluctuations and the oscillations exhibited in shielded thrusters after a mode

transition drive the hypothesis that this instability is a form of the breathing mode.

Provided these oscillations in shielded thrusters are related to the breathing mode, there is no existing theory to explain why they would manifest as a stronger fluctuation at reduced current and high specific impulse. Intriguingly, in the so-called unshielded Hall thruster, the NASA-173Mv2, that was driven to even higher specific impulse and lower currents, a transition to a more intense fluctuation level of breathing mode was not observed.[49] While it is possible this change in stability margin could be attributed to differences in the size and geometry of the 173Mv2 compared to the shielded test articles that exhibited the mode transition, the disparity also invites the possibility that there could be a difference inherent to shielding that impacts the onset of the instability. For example, in shielded thrusters, plasma-wall interactions are drastically reduced, resulting in higher electron temperatures.[3] The plasma discharge is also typically displaced further downstream when compared to unshielded geometries. With that said, while these variations—or other factors—ultimately could dictate if and when different thruster types exhibit strong oscillations, there are to our knowledge no experimentally validated, analytical criteria for mode transitions that would allow us to quantify the influence of these effects.

This lack of analytical criteria for the onset of large amplitude breathing mode oscillations is a major outstanding challenge in the study of Hall thruster dynamics. Indeed, while there is consensus that the breathing mode is ionization-related, the conditions for when this mode is driven unstable remain an active area of investigation. Several theories have been proposed to date about the destabilizing mechanism including that is related to energy balance to the walls,[9,18] ion flux to the anode,[24] nonlinear couplings among the electric field, density, and current,[11,25] and time delay between ionization in the region near the anode vs in the acceleration zone.[10,13,15,47,50] Yet, while many of these previous simulations and theoretical analyses were able to re-create the breathing mode for some operating conditions, there is limited agreement among them about how and why the breathing mode onsets. In order to explain, predict, and ultimately mitigate the mode transition to the heightened oscillations exhibited by shielded thrusters, the need is apparent for a detailed study of this instability's dynamics in these devices.

To this end, the goals of this two part study are (1) to explore the validity of an established simplified model for the breathing mode in unshielded thrusters for describing the oscillations in a shielded device (Part I) and (2) to extract an analytical stability criterion for mode transitions from this model and leverage this criterion to inform strategies for mitigating the mode transition at high discharge voltages (Part II). The model we choose to baseline in this work is based on the efforts of Barral and Peradzyński,[13] as it has been shown to exhibit behavior qualitatively consistent with spatially and time-resolved measurements of fluctuating plasma properties in a magnetically shielded Hall thruster.[47]

This first part is organized in the following way. In Sec. II, we review the model and formulate its key assumptions in terms of experimentally testable criteria. In Sec. III, we convert experimental results from our previous work, Ref. 47, to 0D, spatially averaged quantities that can be compared against the assumptions and predictions of the two-equation model. In Sec. IV, we systematically evaluate the model assumptions with our experimental measurements and directly compare the governing equations to the measured fluctuations. In Sec. IV, we discuss the implications of the validity of the model assumptions and its extensibility.

II. OVERVIEW OF TWO-ZONE, TWO-EQUATION MODEL FOR OSCILLATIONS

We present in this section an overview of the two-zone model based on the result first presented by Barral and Peradzyński.[13] This provides the framework for the experimental validation we present in Sec. III. To this end, we introduce the canonical thruster geometry, define notation for the model's 0D parameters, and overview the key assumptions for the model and resulting governing equations.

A. Thruster geometry

Figure 1 shows a canonical geometry of a Hall thruster cross section. The device consists of an axial electric field, $\vec{E}$, applied across a confining radial magnetic field, $\vec{B}$, in a discharge channel of width, w, average radius, r, and cross-sectional area, $A = 2\pi rw$. Neutral density propagates from an upstream manifold where it is then impact ionized by electrons (not shown) in the plasma. The domain where this occurs is denoted as the "ionization zone." The resulting ions are then accelerated out of the geometry by the applied electric field. This region is denoted as the "acceleration zone" with characteristic length, L, which is qualitatively consistent with the location and extent of the"avalanche region" defined for the Barral model.[13] We adopt the nomenclature "'acceleration zone" for our work given its close correlation with the electric field. The model presented here treats oscillations in the spatially averaged plasma properties in both of these zones. The dynamics in these regions are assumed to be causally connected in the form of propagating perturbations in the neutral density flux and discharge current.

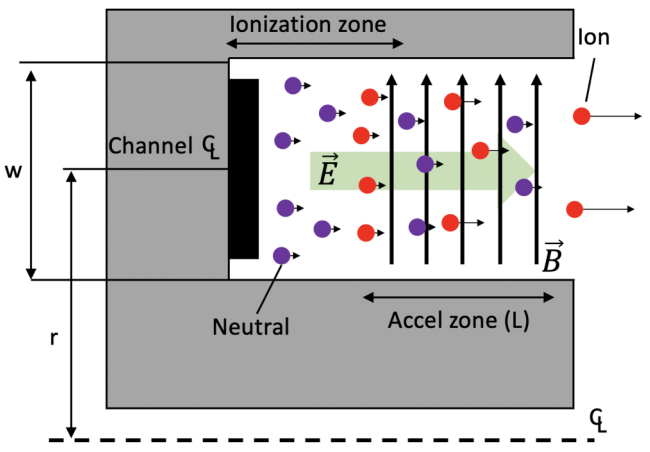

FIG. 1. Cross section of Hall thruster canonical geometry.

B. Notation

We overview in the following the definitions and notation for our analysis that are referenced with respect to the geometry shown in Fig. 1. This nomenclature follows Refs. 13 and 15. Unless otherwise indicated, the units are SI.

- $\bar{x}$ denotes the time-average/steady-state value of quantity x.
- $\tilde{x}$ denotes the time-varying component of quantity x, i.e., $\tilde{x} = x - \bar{x}$.
- n denotes the volumetric average of plasma density in the acceleration zone. Both the ion and electron density are assumed to be the same on the timescale of the oscillations.
- N denotes the volumetric average of neutral density in the acceleration zone.
- T_e denotes the volumetric average of electron temperature in the acceleration zone in units of electron volts.
- E is the volumetric average of electric field in the acceleration zone.
- u_i denotes the volumetric average of axial ion velocity in the acceleration zone.
- u_e denotes the volumetric average of axial electron velocity in the acceleration zone.
- u_D denotes the volumetric average of the relative drift between ions and electrons in the acceleration zone.
- u_n denotes the volumetric average of axial neutral speed in the acceleration zone.
- I denotes the discharge current in the thruster.
- $Q(t)$ denotes the volumetric flow rate of neutrals into the acceleration zone from the upstream ionization zone.
- Q_0 denotes the volumetric flow rate of neutrals from the anode into the ionization zone.
- β denotes the volumetric average of the "electron multiplication" rate in the acceleration zone.[13] This parameter also can be interpreted as a rate coefficient for ionization, which is frequently written as a function of temperature, $\zeta(T_e)$.[51] In this work, we refer to this parameter as a rate coefficient.
- $\gamma = \beta(n/I)$ denotes the volumetric "effective" ionization rate of neutrals in the acceleration zone. It is the ratio of the ionization frequency of neutrals, i.e., the timescale of creation of electrons, divided by the discharge current. It is given in units of $s^{-1}A^{-1}$.
- τ is the transit time of neutrals across the ionization zone to the acceleration zone.
- ν_{loss} represents the rate of loss of electrons to the walls and flowing out of the acceleration zone,

$$\nu_{loss} = c_s \frac{2}{w} - \frac{u_e}{L}. \tag{1}$$

This expression is found from the application of a control volume integral to the continuity equation for electrons where the volume is the acceleration zone. The first term represents losses through the sheath to the non-conducting wall, where $c_s = \sqrt{qT_e/m_i}$ is the ion sound speed, m_i is the ion mass, and q is the fundamental charge. The second term represents the drift of electrons through the channel as a result of cross-field diffusion.

C. Governing equations and key assumptions

The linearized version of the approach in Ref. 13 models the thruster plasma as two 0D regions, the acceleration and ionization zones, described by equations for the volumetrically averaged neutral density and discharge current. The derivation of these governing equations, as outlined in this preceding work, begins with a 1D model in which the non-local nature of the instability is represented.[14] The 1D model is then translated into the two-zone, 0D model[13,15] by leveraging an approach based on considering derivatives of linear operators in 1D space.

Experimentally verifying all the key assumptions underlying this heavily mathematical treatment of linear operators is beyond the experimental capabilities outlined in the present investigation. However, the same form as derived in Refs. 13 and 15 does emerge if a complementary set of key assumptions are invoked about the relationships between the 0D plasma properties in the two zones. The verification of these assumptions is experimentally tractable and thus forms the framework for the validation presented in this investigation. With this in mind, we overview in the following the key simplifications we invoke to arrive at the same governing equations as presented in Refs. 13 and 15.

1. Equation for discharge current

The total discharge current in the channel is the summation of the electron and ion currents,

$$I = Aqnu_D, \tag{2}$$

where we have neglected here for simplicity the contribution of multiply charged species. Differentiating with respect to time yields

$$\frac{dI}{dt} = I\left[\frac{1}{n}\frac{dn}{dt} + \frac{1}{u_D}\frac{du_D}{dt}\right]. \tag{3}$$

We can represent the density term in this equation by invoking continuity for electrons volumetrically averaged over the acceleration zone,

$$\frac{dn}{dt} = \beta n N - \nu_{loss} n. \tag{4}$$

Expanding this relation to first order and substituting into Eq. (3) yields

$$\frac{dI}{dt} = I\bar{\beta}\bar{N}\left[\frac{\tilde{N}}{\bar{N}} + \left(\frac{\tilde{\beta}}{\bar{\beta}} - \frac{\tilde{\nu}_{loss}}{\bar{\nu}_{loss}}\right) + \left(\frac{1}{\bar{\beta}\bar{N}}\right)\frac{1}{u_D}\frac{du_D}{dt}\right], \tag{5}$$

where we have used the steady-state result that $\bar{\beta}\bar{N} = \bar{\nu}_{loss}$, i.e., the time-averaged creation rate of electrons from ionization must be equal to the rate at which electrons flow out of the acceleration zone.

We make two assumptions to simplify Eq. (5):

Assumption 1.1 The contribution of the relative variations in the loss rate, $\tilde{\nu}_{loss}/\bar{\nu}_{loss}$, and rate coefficient, $\tilde{\beta}/\bar{\beta}$, can be neglected.

Assumption 1.2 The ratio of the rate change in drift velocity to the ionization frequency of ions, $\left(\frac{1}{\bar{\beta}\bar{N}}\right)\frac{1}{u_D}\frac{du_D}{dt}$, can be neglected.

Taken together, these assumptions allow us to write

$$\frac{dI}{dt} = I\bar{\beta}[\tilde{N}] = I\bar{\beta}[N - \bar{N}]. \tag{6}$$

This is the same result as presented in Ref. 13 with the exception that we have explicitly defined the time average of the rate coefficient, $\bar{\beta}$. In the nomenclature of Ref. 13, β was defined as not have time-varying components, and so the bar notation was not used for these properties. We have chosen to keep the average notation in our work to facilitate our subsequent experimental analysis. Physically, Eq. (6) reflects the assumption that the dominant driver for changes in the current is the fluctuation in charge carrier production resulting from oscillations in the neutral density and current.

2. Equation for neutral density

We express the 0D continuity equation for neutral density under the assumption that the mass flow of neutrals out of the acceleration zone is negligible compared to the inlet flow,

$$\frac{dN}{dt} = -\beta n N + \frac{Q(t)}{L}. \tag{7}$$

We expand the right side of this expression to first order to find

$$\frac{dN}{dt} = \bar{\beta}\bar{n}N\left[-1 - \frac{\tilde{n}}{\bar{n}} - \frac{\tilde{\beta}}{\bar{\beta}}\right] + \frac{Q(t)}{L}. \tag{8}$$

We can eliminate plasma density in this expression in favor of oscillations in current by considering the first-order relationship for perturbed quantities from Eq. (2): $\tilde{n}/\bar{n} = \tilde{I}/\bar{I} - \tilde{u}_D/\bar{u}_D$. This allows us to write the continuity equation as

$$\frac{dN}{dt} = \bar{\beta}\bar{n}N\left[-1 - \frac{\tilde{I}}{\bar{I}} + \left(\frac{\tilde{u}_D}{\bar{u}_D} - \frac{\tilde{\beta}}{\bar{\beta}}\right)\right] + \frac{Q(t)}{L}. \tag{9}$$

To further simplify this expression, we make the following two assumptions:

Assumption 2.1 The contribution of the relative variations in total drift, $\tilde{u}_D/\bar{u}_D$, and rate coefficient, $\tilde{\beta}/\bar{\beta}$, can be neglected in the quantity.

Assumption 2.2 Consistent with the ansatz proposed in Ref. 13, the inflowing neutral density can be related to the discharge current and average effective ionization rates in the ionization region,

$$Q(t) = Q_0 \exp\left[-\bar{\gamma}\int_{t-\tau}^{t} I(t^*)dt^*\right]. \tag{10}$$

This result stems from the (potentially strong) assumptions that the electron temperature is only weakly varying spatially and in time in the ionization region, that there is a linear scaling between density and current in the ionization region, that recombination at the anode is neglected, and that the neutral speed is constant in this region. We remark here as well that consistent with the assumptions invoked in Ref. 13, the effective ionization rates in the ionization and acceleration zones are assumed to be the same.

Taken together, these assumptions allow us to reduce Eq. (9) to

$$\frac{dN}{dt} = -\bar{\gamma}NI + \frac{Q_0}{L}\exp\left[-\bar{\gamma}\int_{t-\tau}^{t} I(t^*)dt^*\right]. \tag{11}$$

This is the same result as presented in Ref. 13. Physically, it indicates that the dominant drivers for neutral density in the acceleration zone are ionization resulting from fluctuations in current and neutral density (first term on the right side) balanced against changes in the influx of neutrals from the upstream ionization region (second term on the right side). The fluctuations for inflowing neutral density in turn are moderated by time-varying ionization in the ionization zone that depends on the total thruster current and the transit time of neutrals from this region to the acceleration zone.

3. Summary and physical interpretation

The two-equation model represented by Eqs. (6) and (11) reduces the description of the oscillations in the breathing mode to two key properties: fluctuations in neutral density and current. While two-equation models have been applied in previous descriptions of the breathing mode dynamics in the acceleration zone (cf. Ref. 8), the present formulation has the additional fidelity that it incorporates feedback from a spatially distinct region, the ionization zone. There is a direct link between the two zones moderated by the discharge current and the transit time of neutrals from the ionization to acceleration regions. Depending on the relative phasing of characteristic ionization and transit time, the incoming variations in neutral density can either reinforce or interfere with the ongoing ionization-induced oscillations in the neutral density. This can result in the growth and self-sustaining of the oscillation.

The need for feedback from another region to describe accurately the oscillations is consistent with the larger body of work on the breathing mode where it has been suggested that this oscillation is inherently more than zero-dimensional.[13,15,20,24,25] The effective incorporation of the oscillations from the upstream region leads to the description of this model as "two zone."

In practice, this model has several compelling features that recommend it as a potential framework for anticipating mode transitions. First, the model has been shown to be able to produce oscillations in discharge current with properties consistent with the amplitude and frequency exhibited by the breathing mode in Hall thrusters.[13] Second, Barral and Peradzyński[13] have demonstrated through numerical solutions and linear perturbation analysis that for certain assumed background plasma properties, the oscillations anticipated from this model can be damped. This opens the possibility that these equations may be able to anticipate mode transitions. Third, as we have discussed in Ref. 47, experimental measurements indicate that perturbations in neutral density propagate from the ionization zone to the acceleration zone, convecting

on the timescale of the breathing mode oscillation. This is consistent with the key assumption underlying the treatment of the neutral density flux in this model.

With that said, the question remains whether this model and its assumptions are valid for a real magnetically shielded thruster. This motivates the following treatment, in which we employ experimental measurements to investigate systematically each assumption.

III. REVIEW OF TIME-RESOLVED EXPERIMENTAL MEASUREMENTS IN A MAGNETICALLY SHIELDED HALL THRUSTER

We present in this section a review of time and spatially resolved measurements we previously performed in a magnetically shielded thruster undergoing breathing mode oscillations.[47] These measurements ultimately inform our evaluation of the assumptions outlined in Sec. II. To this end, we first show examples of the time evolution of these properties on thruster centerline and then convert these measurements to 0D, spatially averaged quantities.

A. Time-resolved plasma properties along channel centerline

In our previous work,[47] we employed a combination of laser induced fluorescence and a far-field current density probe to characterize the time-resolved plasma and neutral properties along the channel centerline of a Hall thruster (Fig. 1) on the timescale of the breathing mode oscillation. The device in this study was the H9, a magnetically shielded Hall thruster, that we operated at 3 kW discharge power and 300 V discharge voltage. We remark here that this condition did not correspond to the extremely strong manifestation of breathing exhibited at low currents and high specific impulse characteristic of the shielded Hall thruster.[5] However, as we proceed in this work under the assumption that this oscillation is a breathing mode, we still can gain insight into its dynamics by considering this more quiescent condition. In turn, provided we can demonstrate the model is valid for describing the dynamics at this state, our intention in Part II is to leverage the model to anticipate and explain the mode transitions at the highly oscillatory conditions.

The details of the experimental technique can be found in Ref. 47. In brief, the method is based on solving the ion momentum and continuity equations by employing experimentally measured ion flux density and moments of the ion velocity distribution function. These solutions then are coupled with the neutral continuity equation and an electron Ohm's law to yield a set of spatially and time-resolved measurements of plasma and neutral density, electron temperature, rate coefficient, ion and neutral velocity, and electrical field along channel centerline. Figure 2 shows examples of the results of this method where we depict spatiotemporal plots of discharge current, electron temperature, and neutral density. Here, we have shown each property as a function of axial distance along the channel and as a function of phase of the discharge current oscillation. Spatial coordinates have been normalized to channel length and referenced with respect to the exit plane. Our use of phase dependence is a result of the analysis method, which is based on a phase-sensitive transfer function referenced with respect to the discharge current. The frequency of the oscillation was $f_{BM} \sim 16$ kHz. The conversion to time dependence can be effected with the prescription $t = \phi/(360 f_{BM})$ where ϕ is the phase expressed in degrees.

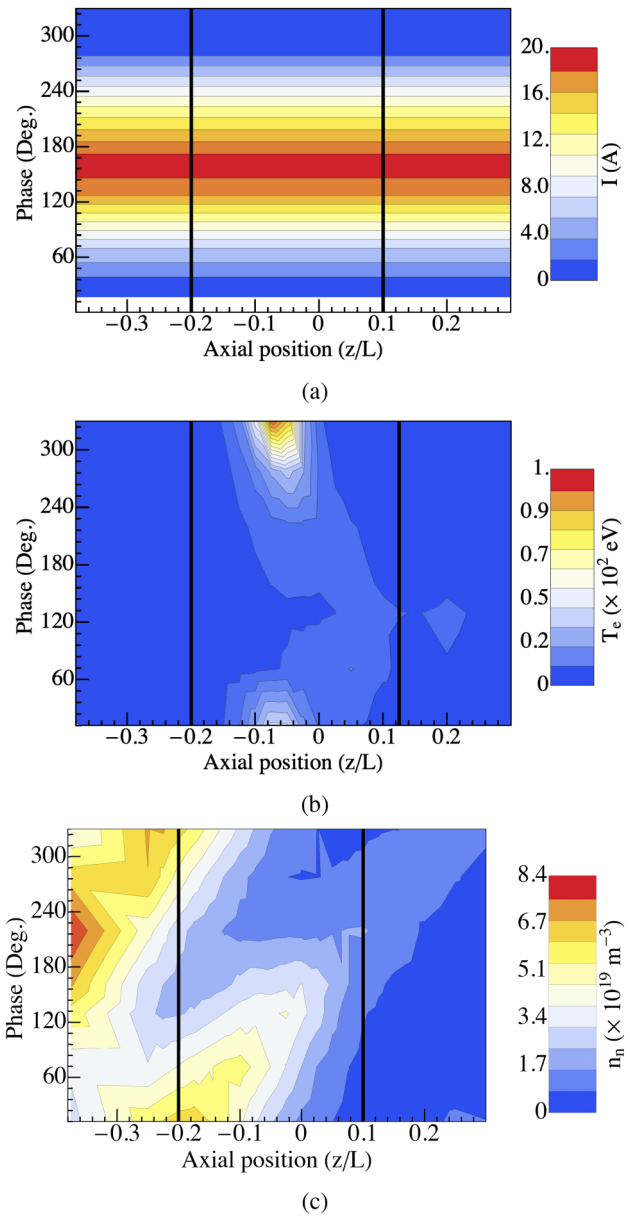

FIG. 2. Contour maps of (a) discharge current, (b) electron temperature, and (c) neutral density along channel centerline as a function of breathing mode phase for the H9 thruster operating at 300 V discharge voltage and 10 A discharge current. The boundaries of the acceleration zone are denoted with vertical lines. Data adapted from Ref. 47 with resolutions of 2 mm spatially and 50° in phase. Lengths are normalized to channel length and referenced to the thruster exit plane.

The plasma properties shown in Fig. 2 all oscillate on the timescale of the breathing mode with the same characteristic frequency. The discharge current in Fig. 2(a) is uniform in the axial direction. This is a result of current continuity in the thruster, which is ensured by the fact that the walls are non-conducting. Physically, this figure emphasizes the fact that current oscillations are non-local in the plasma. The electron temperature shown in Fig. 2(b) also oscillates on the timescale of the discharge current with a waveform characterized by a strong variation in magnitude ($> 50\%$) and a periodic spatial shift confined to a region between $z/L = -0.2 - 0.1$. The spatial variations in electric field (not shown) follow a similar though slightly broader spatial trend. Given the critical role of the temperature profile in driving ionization of ions in the acceleration zone, we use this parameter as our benchmark for defining the bounds of the acceleration zone of interest in the model. We mark the boundaries upstream and downstream of where this property varies spatially and denote it as the "acceleration zone" for the remainder of this work. We note that in adopting this convention, our geometry omits a downstream portion where electric field is finite and ion acceleration continues. However, ionization is negligible in these downstream regions as the electron temperature decreases.

Figure 2(c) shows the time-resolved fluctuations in neutral density. As indicated here and demonstrated in Ref. 47, these oscillations are characterized by the propagation of perturbations downstream at approximately the neutral velocity. Notably, these fluctuations, which are $> 50\%$ of the mean value, have a high amplitude in the region upstream of where we have defined the acceleration zone. As we suggested in Ref. 47, this may indicate these modes are originating in this region. As a high degree of ionization evidently is occurring here, we denote this area, consistent with Fig. 1, as the "ionization region." We note here that the fact that the ionization and acceleration zones appear to be spatially distinct yet fluctuating is a key assumption of the model.

B. Spatially averaged properties

In this section, we convert the 1D time-resolved measurements from Ref. 47 into 0D time-resolved fluctuations in the channel. We accomplish this by spatially averaging the measured plasma properties over the channel centerline in the acceleration zone defined in Fig. 2. Figure 3 displays the time-dependent results for variations in the plasma density, neutral density, axial ion speed, axial electron speed, relative drift, electron temperature, axial electric field, rate coefficient, inflowing volumetric flow rate of neutrals from the ionization zone, and discharge current. We note that in order to infer the average electron speed, which was not measured directly with our technique, we invoked Eq. (2) to estimate $u_e = I/(qnA) + u_i$. We determined the inflowing volumetric flow rate, $Q(t)$, by averaging over the spatial points adjacent to the boundary defined between the ionization and acceleration zones. We do not depict the neutral velocity, as this was approximately constant over the period of oscillation. In all cases, we have included credible intervals to reflect uncertainty in the measurement. This stems from a reported uncertainty in phase of $\pm 27°$[47] and an average assumed 15% uncertainty in the plasma property value. We base this latter value on the typical uncertainty bounds reported in previous work for the plasma properties,[47] which were inferred from a bootstrapping analysis.

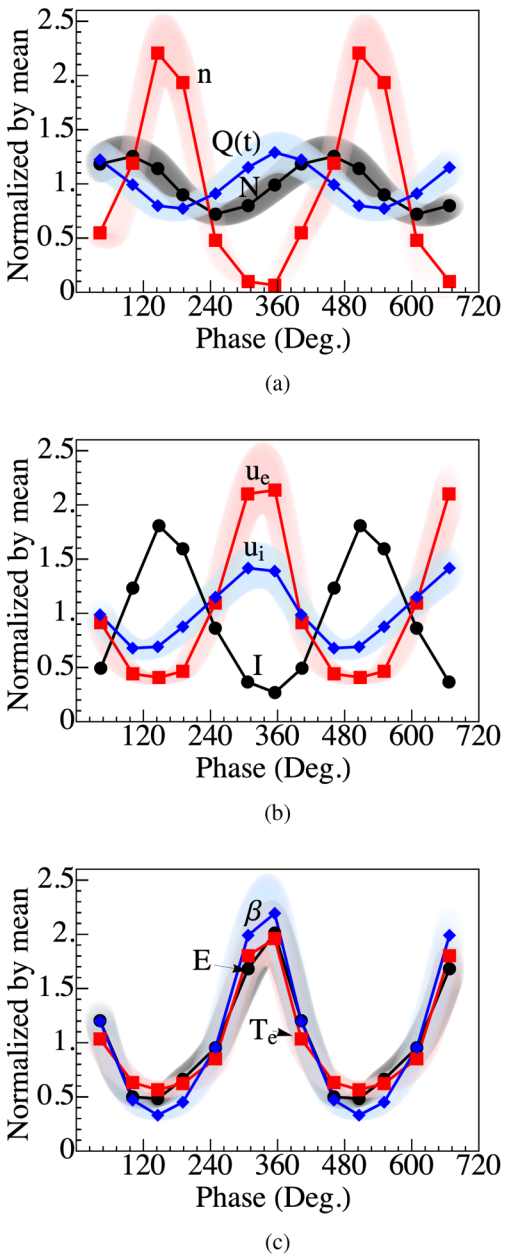

FIG. 3. Plasma properties averaged spatially over the acceleration zone as a function of phase in the breathing mode. All data have been normalized by the mean values: $\bar{n}_e = 6.9 \times 10^{17}$ m^{-3}, $\bar{Q} = 4.3 \times 10^{21}$ m^{-2}s^{-1}, $\bar{u}_e = -26$ km/s, $\bar{u}_i = 4.8$ km/s, $\bar{I}_D = 10$ A, $\bar{\beta} = 3.2 \times 10^{-14}$ m^{3}s^{-1}, $\bar{T}_e = 9.7$ eV, and $\bar{E} = 11.8$ kV/m.

The results in Fig. 3 illustrate that all plasma quantities oscillate on the timescale of the breathing mode but with different

relative phasing. For example, the ion drift, opposite of the electron drift, total drift, electron temperature, and ionization rate coefficient are approximately in phase with the electric field. Qualitatively, the correlation with ion drift is expected, as the electric field is the dominant driving force for ion acceleration. Similarly, the correlation between the opposite of electron drift and electric field can be explained from a first order consideration of the generalized Ohm's law.[51] The correspondence between electric field and total drift, $u_D = u_i - u_e$ results from the in-phase relationship between both species' speed and the electric field. The relationship between electric field and temperature may in part be explained qualitatively given that the primary source of electron thermal energy in the channel is Ohmic heating. The correlation between electric field and rate coefficient stems from the monotonic dependence of this latter term on electron temperature, cf. Ref. 51.

We also see from Fig. 3 that the discharge current is anti-correlated with the relative species drift while it is strongly correlated with the plasma density. This suggests that it is the variations in the number of charge carriers rather than variation of the species' speeds that is the driving factor for fluctuations in current. Relatedly, the neutral density fluctuations lead the oscillations in current. This out of phase—but not fully anti-correlated—relationship is characteristic of the typical "predator–prey" interpretation of the breathing mode.[8] We also note that the influx from the volumetric flow rate from the ionization zone, $Q(t)$, is anti-correlated with the neutral density fluctuations. As we examine in the following, this phasing can help promote and reinforce the oscillations in the acceleration zone.

IV. EXPERIMENTAL EVALUATION OF MODEL

Now that we have established experimentally the spatially averaged plasma properties, we can evaluate the key assumptions for the governing equations for discharge current and neutral density outlined in Sec. II.

A. Assumptions for equation for discharge current

We show in Figs. 4(a) and 4(b) the terms in the quantity on the right side of Eq. (5) over two breathing mode cycles. We have propagated uncertainty from the experimental measurements to these results by following standard prescriptions for addition, multiplication, and division.[52] The trends shown in Fig. 4(a) at first would suggest that Assumption 1.1 is not justified. The relative magnitude of variations in the loss rate and ionization rate coefficient have larger amplitudes compared to the variations in neutral density and drift speed. As can be seen, however, the shape and magnitude of these first two terms are identical within uncertainty over the breathing mode cycle. As a result, their total contribution in the context of Eq. (5) cancels. Assumption 1.1 thus is in effect approximately satisfied. Physically, this negation of the two dominant terms could be explained by the strong dependence of both the electron temperature (and thus rate coefficient) and electron drift (correlated with the loss term) on variations in the electric field. We return to this point in Sec. V.

The trends in Fig. 4(b) indicate that Assumption 1.2, in which we neglect the relative variation in drift speed in Eq. (5), is not strongly satisfied. Given that Assumption 1.1 allows us to ignore the second quantity in Eq. (5), the only way in which Assumption 1.2 would be valid is if the relative drift speed term were small compared to the relative variation in neutral density. However, we see from Fig. 4(b) that although the amplitude of the relative drift is smaller, it is not negligible compared to the relative neutral density's amplitude.

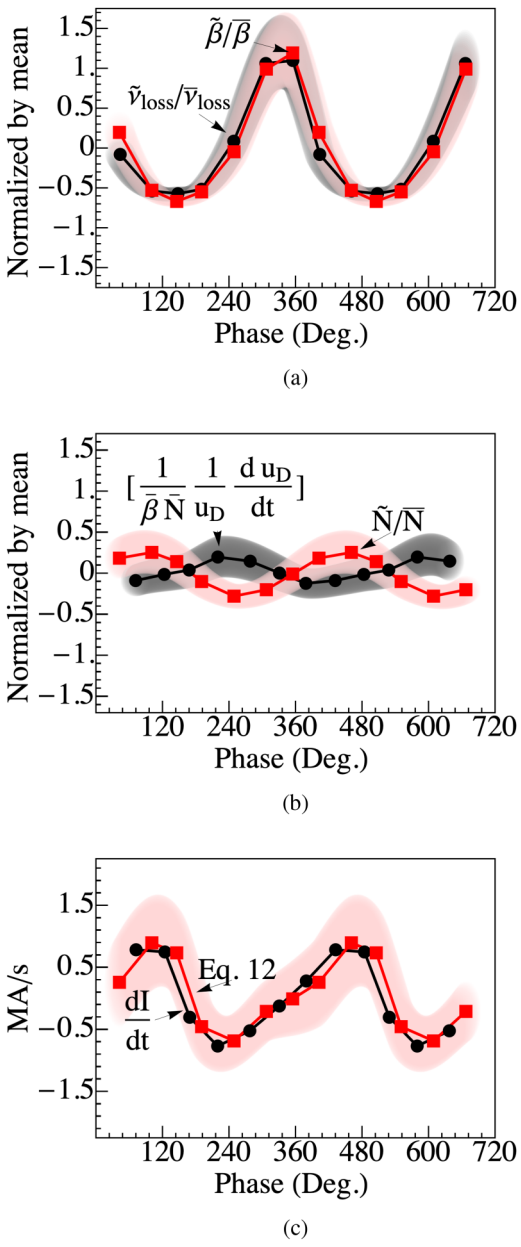

FIG. 4. (a) and (b) Relative variations in quantities relevant to Assumption 1. (c) Derivative of discharge current compared to the model's equation for the derivative of discharge current, Eq. (12) with $c = 0.5$.

With that said, we note that the two quantities are 180° out of phase such that we can represent their relationship symbolically as $\tilde{u}_D = -c\tilde{N}$ where c is a constant less than unity. In practice, if we make the strong assumption motivated by this empirical observation that the relative phasing in neutral density and drift velocity remains 180 degrees out of phase, we can still recover a version of Eq. (6) with a modification,

$$\frac{dI}{dt} = (1 - c)I\bar{\beta}[N - \bar{N}]. \tag{12}$$

We show the left and right sides of this expression in Fig. 4(c) with a factor of $c = 0.5$. While there are minor differences in phase at the maxima in these trends, overall, the close agreement in the result provides validation for this modified governing equation. Moreover, the magnitude of the correction in turn suggests the original proposed governing relationship, Eq. (6), is valid within a factor of unity. In practice, the reason why the neutral density and rate change in discharge current are anti-correlated may in part be attributed to the impact of ionization on the momenta of the ions and electrons. We return to this point in the discussion.

In summary, the experimental results suggest that the assumptions underlying the simplified form of Eq. (6) are approximately validated for this thruster operating condition.

B. Assumptions for equation for neutral density

We show in Fig. 5(a) two terms in the quantity of Eq. (9), $\tilde{u}_D/\bar{u}_D$ and $\tilde{\beta}/\bar{\beta}$. While the variations of the individual properties are non-negligible in time, they are identical within errors such that, as with Assumption 1.1, the terms cancel in Eq. (9). This supports Assumption 2.1. Qualitatively, this result can be understood by recognizing both drift speed and ionization rate are strongly correlated with electric field.

Figure 5(b) shows a comparison of the measured inlet volumetric flow rate, $Q(t)$, and the proposed analytical form from Eq. (10) in Assumption 2.2. To generate this result, we have used the average effective ionization rate of $\gamma = 2100\,\mathrm{s}^{-1}\,\mathrm{A}^{-1}$ based on measured plasma values and an assumed neutral transit time of $\tau = 21\,\mu\mathrm{s}$. We found the latter value by adjusting it parametrically until we achieved the best agreement between the proposed analytical and measured inlet volumetric rates. We note that this value is consistent with ionization zone lengths on the order of 0.5–1 cm and neutral speeds on the order of 200–400 m/s, which are expected for this test article. As can be seen from the result in Fig. 5(b), the assumed form for the inlet flux and the measured quantity agree in amplitude and phase within experimental uncertainty. This validates Assumption 2.2 for this operating condition. Given that both key assumptions thus are satisfied, we proceed to show in Fig. 5(c) the left and right sides of Eq. (11). The magnitude and phase of the oscillations align within uncertainty, lending confidence to this simplified expression for the neutral dynamics.

In summary, we have shown in the preceding that the key assumptions for reducing the description of the dynamics of the breathing mode to two equations representing fluctuations in current and neutral density are largely satisfied. Moreover, we have shown that the resulting equations represent the underlying measured dynamics. We expand on the implications of this result in the following.

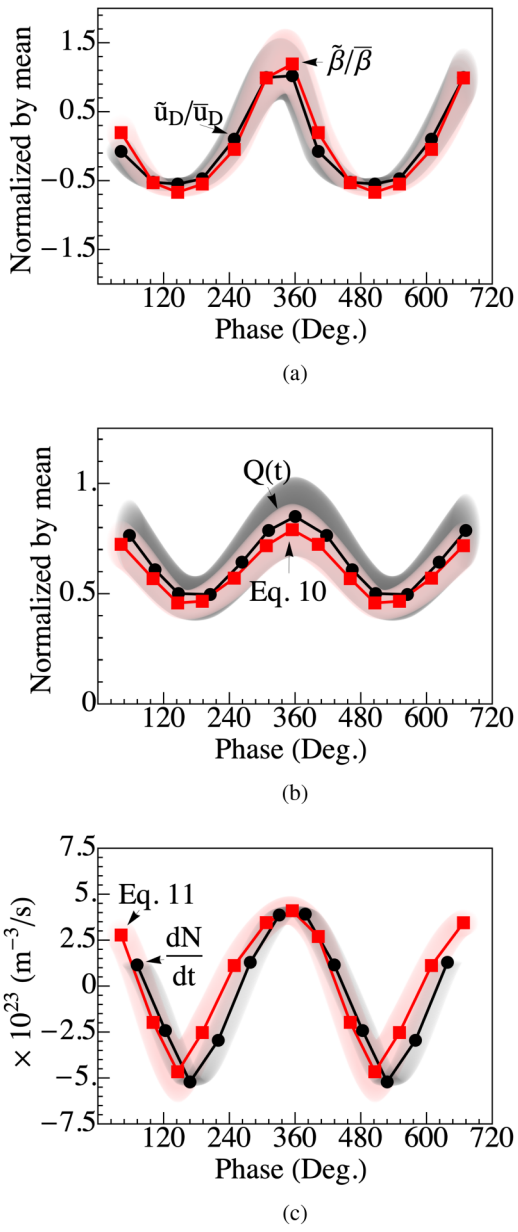

FIG. 5. (a) and (b) Relative variations in quantities relevant to Assumption 2. (c) Derivative of neutral density compared to the model's equation for the derivative of neutral density, Eq. (11).

V. DISCUSSION

We discuss in this section the physical significance of the key assumptions we have invoked, the challenges with model

extensibility, and the implications of this result for predicting mode transitions.

A. Physical interpretation of the assumptions

The key simplifying feature of the model evaluated in this work is that it expresses the dynamics of the breathing mode in terms of only two oscillating quantities, the volumetrically averaged neutral density and discharge current. The mode thus can be described with two equations that govern fluctuations in these properties. In arriving at these expressions, it has been necessary to neglect contributions from fluctuations in other plasma properties including the speeds of the species, electric field magnitude, and electron temperature. Given the large amplitude of the breathing mode, however, we would not anticipate that these other plasma quantities should not vary. And indeed, our experimental measurements have shown that not only do properties like the loss rate and relative drift fluctuate on the timescale of the breathing mode but that their relative amplitudes (Figs. 4 and 5) are comparable to or larger than fluctuations in the neutral density and discharge current. This suggests that eliminating these terms strictly on the grounds that their relative variations are negligible is not justified. With that said, our results do show that due to convenient cancellations in terms, the influence of parameters other than variations in the density and discharge current can in practice be neglected for the specific test case under investigation. We discuss here possible physical reasons for why these properties have this effective balancing.

1. Balance between ionization rate, loss, and drift terms

The strong correlation in phase among the relative drift, loss, and rate coefficient may in part be explained by the fact that all of these parameters are directly driven by the electric field. We can motivate this dependence qualitatively for each parameter by considering the momentum and energy flux in the thruster.

To elucidate the relationship between field and relative drift, we consider momentum scaling for both the ions and electrons. For ion drift, the in-phase relationship with electric field suggests that the acceleration from this field occurs nearly instantaneously on the timescale of the breathing mode oscillation. Qualitatively, this is justified given that the characteristic transit time in the channel, u_i/L, is an order magnitude faster than the breathing mode cycle. Quantitatively, we have indeed observed in our previous work[47] that perturbations of the ions propagate more quickly than the timescale of the oscillation. For the electron drift speed, the in-phase relationship with electric field may qualitatively be understood from a generalized Ohm's law.[51] To zeroth order, if we neglect the action of the pressure gradient, this relationship indicates that the axial electron drift scales with electric field per $-u_e \propto E\nu_e$ where ν_e is the effective electron collision frequency in the channel. We introduce this scaling with the caveat that the actual relationship between electric field and drift is likely more nuanced as it has been shown that the collision frequency in practice is non-classical and dynamic in the thruster channel.[43] With that said, taken together, the relative anticipated relationship of ion and electric drift speeds with electric field can motivate why the relative drift between these species exhibits the strong correlation with field that we observed.

The correlation between the loss term [Eq. (1)] and electric field can be explained by considering the two contributions to this expression, the drift speed and the ion sound speed. For the electron drift speed, the previous argument related to the Ohm's law qualitatively justifies why this contribution to the loss term scales with electric field. For the ion sound speed, its relationship to electric field stems from its dependence on temperature, which in turn can be related to electric field by considering an electron energy equation. In practice, this governing relation contains several factors including non-classical heat flux, conduction, Ohmic heating, and energy losses due to ionization. With that said, qualitatively, a dominant driver for introducing energy to the plasma, and by extension the electron temperature, is Ohmic heating arising from the electric field. Similarly, in a 0D sense, convection is a dominant effect for removing energy from the volume. By balancing convection and Ohmic heating, we can recover $T_e \propto E$, i.e., a direct correlation between temperature and field. This scaling coupled with the relationship between electron drift and electric field motivates qualitatively why the overall loss term is strongly correlated with the electric field.

Finally, we note that the variation in rate coefficient with electric field can be justified on the same grounds as the electron temperature. Indeed, this quantity exhibits a monotonic dependence on this plasma property.

In summary, there are qualitative arguments informed by a consideration of higher fidelity transport equations for why the relative drift, loss, and ionization rate all should scale with the electric field and thus exhibit the strong correlation in phase that we have observed. With that said, more quantitatively, we cannot with this fidelity of description explain why the variation in these quantities almost exactly cancel in the governing relations. Physically, our observation that these terms do counterbalance can be interpreted as the fact that any increase in charge carriers in the acceleration zone driven by changes in Ohmic heating is balanced by enhanced losses of these charge carriers from the acceleration zone by increased drift/Bohm speed resulting from the enhanced electric field. Showing from first principles why this balance holds would require a detailed consideration of the higher fidelity representation of the dynamics, including a treatment of the non-classical transport coefficient. This is beyond the scope of this work.

In practice, our experimental results show that at least for this operating condition, this balance allows us to neglect the variations in these other plasma quantities in a formulation for the breathing mode.

2. Inverse relationship between drift speed and neutral density

As discussed in Sec. IV, Assumption 1.2 concerning the neglect of the rate change in drift velocity is indirectly satisfied by the observation that this parameter is anti-correlated with and has a smaller amplitude than the relative fluctuations in neutral density. In practice, the result is that for our operating conditions, the amplitude of the neutral density fluctuations in the simplified equation, Eq. (12) is modified by a factor less than one.

Physically, the relationship between neutral density and the rate change in relative drift may in part be explained by considering the influence of ionization on electron and ion drifts. Indeed, qualitatively, the result of an ionization event is to add a new particle with no effective drift to a given species. Ionization thus can be interpreted as lowering the magnitude of the drift speed for each species at the ionization frequency. We thus may anticipate qualitatively an anti-correlation between neutral density—a dominant driver for ionization—and each drift speed, as indicated experimentally from our results. This conclusion is tempered of course by the fact that electric field, non-classical collision frequency, and pressure also will influence the net drift speeds.

The reason why only a moderate correction (50%) is needed to account for the drift fluctuations may be qualitatively understood by the form of the relative drift term, which scales as $\nu_{ion}^{-1}[u_D^{-1}du_D/dt]$, the ratio of the inverse timescale of fluctuations in drift speed compared to the ionization frequency of ions. The ionization timescale is on the order of 500 kHz while the rate change in the drift speed is on the order of the angular frequency of the breathing mode, 100 kHz.

B. Extensibility of model

We have shown in this work that experimental measurements indicate the key assumptions, 1.1, 1.2, 2.1, and 2.2, for the simplified two-equation model are approximately satisfied. In practice, however, we can only definitively claim that these assumptions informed by our experimental measurements are valid for this specific operating condition, 300 V discharge voltage and 10 A discharge current. This invites the key question as to how extensible the model is to other operating conditions for the thruster.

Based on the preceding discussion, we may expect that elements of these assumptions may be valid beyond the specific case considered here. Indeed, we may anticipate based on these previous arguments that key terms like the loss rate, relative drift, and rate coefficient generally will still exhibit strong correlation with electric field at other operating conditions. However, we have not shown that the convenient canceling of terms that we have observed for this operating condition should persist at different throttle points. Verifying this explicitly would require the same type of detailed comparison of internal plasma properties we have done here over an expanded range of operating conditions. This is beyond the scope of this investigation. With that said, there are key quantities of interest that the model does output, such as amplitude and frequency of oscillation in discharge current, that can be more easily compared parametrically with experimental measurements. Demonstrating the model can anticipate changes in these properties with operating condition thus can serve as an evaluation of its extensibility.

To this point, we note this model has features that may enable it to capture key trends related to mode transitions. Indeed, as discussed in Sec. II C 3, the onset of the instability anticipated in this model depends on the relative scale of ionization frequency and neutral transit time. As both of these properties are functions of operating condition of the thruster, we anticipate that the model may have the versatility to re-ceate mode transitions. With this in mind, a key goal for Part II of this study is to evaluate the extensibility of the model by comparing its outputs to experimental measurements of discharge current oscillations and mode transitions over a wide range of operating conditions.

VI. CONCLUSION

In summary, in Part I of this study, we have employed experimental measurements to evaluate a two-zone model for breathing mode-like oscillations applied to a magnetically shielded Hall thruster. This work is motivated by the need to explain mode transitions in this type of thruster exhibited at high specific impulse (discharge voltage) and low discharge current operating conditions. We have baselined for comparison the model of Barral and Peradzyński[13] as it has the benefits of simplicity but also captures in a simplified way the non-localized nature of ionization-driven oscillations in the device. We have shown through experimental measurement that the assumptions underlying this model are approximately satisfied for this thruster at the investigated operating condition. In effect, only governing equations for oscillations in discharge current and neutral density are necessary to describe the mode. Notably, several other plasma properties such as temperature, drift speed, and electric field also oscillate on the timescale of the fluctuations, but due to the relative phasing of these quantities, their influence can be neglected.

We have discussed qualitatively by invoking scaling arguments from energy and momentum conservation about why these phasing relationships result in this net effect. Though, we have included the caveat that a more detailed examination of the relationship between these quantities would require a higher fidelity theoretical treatment. We have discussed the limitations and implications of our results in the context of the fact that the validation of the model assumptions was only performed for one operating condition. This invites questions about the extensibility of the model to new regimes. To this end, Part II of this effort seeks to assess parametrically the ability of this model to represent the discharge current oscillations in a shielded thruster over a wide range of discharge voltages and currents. In turn, we leverage the model to motivate an analytical stability criterion for mode transitions and to explore hypotheses for why shielded thrusters appear to exhibit mode onset at high discharge voltage and low discharge current operating conditions whereas unshielded thrusters do not.

ACKNOWLEDGMENTS

This work was supported through a Strategic University Research Partnership grant from the California Institute of Technology's Jet Propulsion Laboratory. A portion of the research described here was carried out at the Jet Propulsion Laboratory, California Institute of Technology, under a contract with the National Aeronautics and Space Administration (No. 80NM0018D0004).

AUTHOR DECLARATIONS

Conflict of Interest

The authors have no conflicts to disclose.

Author Contributions

Benjamin A. Jorns: Conceptualization (lead); Data curation (equal); Formal analysis (lead); Funding acquisition (equal); Investigation (lead); Methodology (lead); Project administration (equal); Resources (lead); Writing – original draft (lead). **Ethan Dale:** Data curation (equal); Investigation (equal); Methodology (supporting). **Richard R. Hofer:** Conceptualization (supporting); Funding acquisition (equal); Methodology (supporting); Project administration (equal).

DATA AVAILABILITY

The data that support the findings of this study are available from the corresponding author upon reasonable request.

REFERENCES

[1]I. G. Mikellides, I. Katz, R. R. Hofer, D. M. Goebel, K. De Grys, and A. Mathers, "Magnetic shielding of the channel walls in a Hall plasma accelerator," Phys. Plasmas **18**, 033501 (2011).

[2]I. G. Mikellides, I. Katz, R. R. Hofer, and D. M. Goebel, "Magnetic shielding of a laboratory Hall thruster. I. Theory and validation," J. Appl. Phys. **115**, 043303 (2014).

[3]R. R. Hofer, D. M. Goebel, I. G. Mikellides, and I. Katz, "Magnetic shielding of a laboratory Hall thruster. II. Experiments," J. Appl. Phys. **115**, 043304 (2014).

[4]R. R. Hofer, H. Kamhawi, I. Mikellides, D. Herman, J. Polk, W. Huang, J. Yim, J. Myers, and R. Shastry, "Design methodology and scaling of the 12.5 kW HERMeS Hall thruster for the Solar Electric Propulsion Technology Demonstration Mission," in *62nd JANNAF Propulsion Meeting, Nashville, TN* (JANNAF Interagency Propulsion Committee, 2015), JANNAF-2015-3946.

[5]R. R. Hofer, J. E. Polk, M. J. Sekerak, I. G. Mikellides, H. Kamhawi, T. R. Sarver-Verhey, D. A. Herman, and G. Williams, "The 12.5 kW Hall effect rocket with magnetic shielding (HERMeS) for the Asteroid Redirect Robotic Mission," in *52nd AIAA/SAE/ASEE Joint Propulsion Conference, Salt Lake City, UT* (American Institute of Aeronautics and Astronautics, 2016), AIAA-2016-4825.

[6]E. Y. Choueiri, "Plasma oscillations in Hall thrusters," Phys. Plasmas **8**, 1411–1426 (2001).

[7]J.-P. Boeuf, "Tutorial: Physics and modeling of Hall thrusters," J. Appl. Phys. **121**, 11101 (2017).

[8]J. Fife, M. Martinez-Sanchez, J. Szabo, J. Fife, M. Martinez-Sanchez, and J. Szabo, "A numerical study of low-frequency discharge oscillations in Hall thrusters," in *33rd Joint Propulsion Conference and Exhibit, Seattle, WA* (American Institute of Aeronautics and Astronauticss, 1997), AIAA-1997-3052.

[9]J. P. Boeuf and L. Garrigues, "Low frequency oscillations in a stationary plasma thruster," J. Appl. Phys. **84**, 3541–3554 (1998).

[10]S. Barral, V. Lapuerta, A. Sancho, and E. Ahedo, "Numerical investigation of low-frequency longitudinal oscillations in Hall thrusters," in *29th International Electric Propulsion Conference, Princeton, NJ* (Electric Rocket Propulsion Society, 2005), IEPC-2005-120.

[11]S. Chable and F. Rogier, "Numerical investigation and modeling of stationary plasma thruster low frequency oscillations," Phys. Plasmas **12**, 1–9 (2005).

[12]S. Barral, E. Ahedo, H.-J. Hartfuss, M. Dudeck, J. Musielok, and M. J. Sadowski, "On the origin of low frequency oscillations in Hall thrusters," AIP Conf. Proc. **993**, 439–442 (2008).

[13]S. Barral and Z. Peradzyński, "A new breath for the breathing mode," in *31st International Electric Propulsion Conference, Ann Arbor, MI* (Electric Rocket Propulsion Society, 2009), IEPC-2009-070.

[14]S. Barral and E. Ahedo, "Low-frequency model of breathing oscillations in Hall discharges," Phys. Rev. E **79**, 46401 (2009).

[15]S. Barral and Z. Peradzyński, "Ionization oscillations in Hall accelerators," Phys. Plasmas **17**, 14505 (2010).

[16]S. Barral and J. Miedzik, "Numerical investigation of closed-loop control for Hall accelerators," J. Appl. Phys. **109**, 013302 (2011).

[17]K. Hara, M. J. Sekerak, I. D. Boyd, and A. D. Gallimore, "Mode transition of a Hall thruster discharge plasma," J. Appl. Phys. **115**, 203304 (2014).

[18]K. Hara, M. J. Sekerak, I. D. Boyd, and A. D. Gallimore, "Perturbation analysis of ionization oscillations in Hall effect thrusters," Phys. Plasmas **21**, 122103 (2014).

[19]O. Koshkarov, A. I. Smolyakov, I. V. Romadanov, O. Chapurin, M. V. Umansky, Y. Raitses, and I. D. Kaganovich, "Current flow instability and nonlinear structures in dissipative two-fluid plasmas," Phys. Plasmas **25**, 011604 (2018).

[20]E. T. Dale, B. Jorns, and K. Hara, "Numerical investigation of the stability criteria for the breathing mode in Hall effect thrusters," in *35th International Electric Propulsion Conference, Atlanta, GA* (Electric Rocket Propulsion Society, 2017), IEPC-2017-265.

[21]E. T. Dale and B. A. Jorns, "Two-zone Hall thruster breathing mode mechanism, Part I: Theory," in *36th International Electric Propulsion Conference, Vienna, Austria* (Electric Rocket Propulsion Society, 2019), IEPC-2019-354.

[22]A. Smolyakov, I. Romadanov, O. Chapurin, Y. Raitses, G. Hagelaar, and J. P. Boeuf, "Stationary profiles and axial mode oscillations in hall thrusters," in *2019 AIAA Propulsion and Energy Forum and Exposition, Indianapolis* (American Institute of Aeronautics and Astronautics, 2019), AIAA-2019-4080.

[23]I. V. Romadanov, A. I. Smolyakov, E. A. Sorokina, V. V. Andreev, and N. A. Marusov, "Stability of ion flow and role of boundary conditions in a simplified model of the E × B plasma accelerator with a uniform electron mobility," Plasma. Phys. Rep. **46**, 363–373 (2020).

[24]O. Chapurin, A. I. Smolyakov, G. Hagelaar, and Y. Raitses, "On the mechanism of ionization oscillations in Hall thrusters," J. Appl. Phys. **129**, 233307 (2021).

[25]T. Lafleur, P. Chabert, and A. Bourdon, "The origin of the breathing mode in Hall thrusters and its stabilization," J. Appl. Phys. **130**, 053305 (2021).

[26]L. Leporini, V. Giannetti, M. M. Saravia, F. Califano, S. Camarri, and T. Andreussi, "On the onset of breathing mode in Hall thrusters and the role of electron mobility fluctuations," Front. Phys. **10**, 1–8 (2022).

[27]F. Petronio, A. Alvarez Laguna, A. Bourdon, and P. Chabert, "Study of the breathing mode development in Hall thrusters using hybrid simulations," J. Appl. Phys. **135**, 73301 (2024).

[28]J. Perales-Díaz, A. Domínguez-Vázquez, P. Fajardo, and E. Ahedo, "Simulations of driven breathing modes of a magnetically shielded Hall thruster," Plasma Sources Sci. Technol. **32**, 75011 (2023).

[29]L. Leporini, V. Giannetti, S. Camarri, and T. Andreussi, "An unstable 0D model of ionization oscillations in Hall thruster plasmas," Front. Phys. **10**, 1–7 (2023).

[30]Y. Esipchuk, A. Morozov, G. Tilinin, and A. Trofimov, "Plasma oscillations in closed-drift accelerators with an extended acceleration zone," Sov. Phys. Tech. Phys **18**(7), 928–932 (1974).

[31]F. Darnon, M. Lyszyk, A. Bouchoule, F. Darnon, M. Lyszyk, and A. Bouchoule, "Optical investigation on plasma investigations of SPT thrusters," in *33rd Joint Propulsion Conference and Exhibit, Seattle, WA* (American Institute of Aeronautics and Astronautics, 1997), AIAA-1997-3051 .

[32]K. Polzin, E. Scooby, Y. Raitses, E. Merino, and N. J. Fisch, "Discharge oscillations in a permanent magnet cylindrical Hall-effect thruster," in *31st International Electric Propulsion Conference, Ann Arbor, MI* (Electric Rocket Propulsion Society, 2009), IEPC-2009-122.

[33]R. B. Lobbia, "A time-resolved investigation of the Hall thruster breathing mode," Ph.D. dissertation (University of Michigan, 2010).

[34]M. Sekerak, M. McDonald, R. Hofer, and A. Gallimore, "Hall thruster plume measurements from high-speed dual Langmuir probes with ion saturation reference," in *IEEE Aerospace Conference Proceedings* (IEEE, 2013).

[35]M. S. McDonald and A. D. Gallimore, "Comparison of breathing and spoke mode strength in the H6 Hall thruster using high speed imaging," in *33rd*

International Electric Propulsion Conference, Washington, DC (Electric Rocket Propulsion Society, 2013), IEPC-2013-353.
[36]M. Sekerak, B. Longmier, A. Gallimore, W. Huang, H. Kamhawi, R. Hofer, B. Jorns, and J. Polk, "Mode transitions in magnetically shielded Hall effect thrusters," in *50th AIAA/ASME/SAE/ASEE Joint Propulsion Conference* (American Institute of Aeronautics and Astronautics, 2014), AIAA 2014-3511.
[37]C. J. Durot, A. D. Gallimore, and T. B. Smith, "Validation and evaluation of a novel time-resolved laser-induced fluorescence technique," Rev. Sci. Instrum. **85**, 013508 (2014).
[38]A. Lucca Fabris, C. V. Young, and M. A. Cappelli, "Time-resolved laser-induced fluorescence measurement of ion and neutral dynamics in a Hall thruster during ionization oscillations," J. Appl. Phys. **118**, 233301 (2015).
[39]W. Huang, H. Kamhawi, and T. Haag, "Plasma oscillation characterization of NASA's HERMeS Hall thruster via high speed imaging," in *52nd AIAA/SAE/ASEE Joint Propulsion Conference, Salt Lake City, UT* (American Institute of Aeronautics and Astronautics, 2016), AIAA-2016-4829.
[40]C. V. Young, A. L. Fabris, N. A. Macdonald-Tenenbaum, W. A. Hargus, and M. A. Cappelli, "Time-resolved laser-induced fluorescence diagnostics for electric propulsion and their application to breathing mode dynamics," Plasma Sources Sci. Technol. **27**, 094004 (2018).
[41]I. Romadanov, Y. Raitses, and A. Smolyakov, "Hall thruster with externally driven breathing oscillations," Plasma Sources Sci. Technol. **27**, 4078 (2018).
[42]E. T. Dale and B. A. Jorns, "Non-invasive characterization of the ionization region of a Hall effect thruster," in *54th AIAA Joint Propulsion Conference, Cincinnati, OH* (American Institute of Aeronautics and Astronautics, 2018), pp. 2018–4508.
[43]E. T. Dale and B. Jorns, "Non-invasive time-resolved measurements of anomalous collision frequency in a Hall thruster," Phys. Plasmas **26**, 013516 (2019).
[44]V. H. Chaplin, R. B. Lobbia, A. Lopez Ortega, I. G. Mikellides, R. R. Hofer, J. E. Polk, and A. J. Friss, "Time-resolved ion velocity measurements in a high-power Hall thruster using laser-induced fluorescence with transfer function averaging," Appl. Phys. Lett. **116**, 234107 (2020).
[45]V. Giannetti, M. M. Saravia, and T. Andreussi, "Measurement of the breathing mode oscillations in Hall thruster plasmas with a fast-diving triple Langmuir probe," Phys. Plasmas **27**, 123502 (2020).
[46]P. J. Roberts, V. H. Chaplin, A. Lopez Ortega, and I. G. Mikellides, "Impact of low-frequency oscillations on ion energy in a high-power magnetically shielded Hall thruster," J. Appl. Phys. **131**, 033301 (2022).
[47]E. T. Dale and B. A. Jorns, "Experimental characterization of Hall thruster breathing mode dynamics," J. Appl. Phys. **130**, 133302 (2021).
[48]V. Giannetti, M. M. Saravia, L. Leporini, S. Camarri, and T. Andreussi, "Numerical and experimental investigation of longitudinal oscillations in Hall thrusters," Aerospace **8**, 1–23 (2021).
[49]R. R. Hofer, R. S. Jankovsky, and A. D. Gallimore, "High-specific impulse Hall thrusters, part 1: Influence of current density and magnetic field," J. Propul. Power **22**, 721–731 (2006).
[50]E. T. Dale and B. A. Jorns, "Frequency scaling of the hall thruster breathing mode," in *2019 AIAA Propulsion and Energy Forum and Exposition* (American Institute of Aeronautics and Astronautics, 2019), AIAA-2019-4076.
[51]D. M. Goebel and I. Katz, "Fundamentals of electric propulsion: Ion and Hall thrusters," in *JPL Space Science and Technology Series* (John Wiley & Sons, 2008), p. 508.
[52]H. Ku, "Notes on the use of propagation of error formulas," J. Res. Natl. Bur. Stand., Sec. C: Eng. Instrum. **70C**, 263 (1966).